INVESTIGATING PROLATE–OBLATE SHAPE INVERSION IN Pt NUCLEI NEAR $A \sim 188$*

S.K. Chamoli[a], Aman Rohilla[a], C.K. Gupta[a], R.P. Singh[b]
S. Muralithar[b], S. Chakraborty[c], H.P. Sharma[c], A. Kumar[d]
I.M. Govil[d], D.C. Biswas[e]

[a]Department of Physics and Astrophysics, University of Delhi
New Delhi-110007, India
[b]Inter University Accelerator Centre, Aruna Asaf Ali Marg
New Delhi-110067, India
[c]Department of Physics, Banaras Hindu University, Varanasi (U.P.)-221005, India
[d]Department of Physics, Panjab University, Chandigarh-160014, India
[e]Nuclear Physics Division, Bhabha Atomic Research Center
Trombay, Mumbai-400085, India

(Received January 19, 2017)

Lifetimes have been measured of the low- and intermediate-spins states in ^{188}Pt nucleus using the recoil distance Doppler shift technique at IUAC, Delhi. The nuclear states of interest were populated via ^{174}Yb(^{18}O,4n)^{188}Pt reaction at a beam energy of 79 MeV provided by 15 UD Pelletron accelerator. The extracted B(E2) values show an increase up to 4^+ state and then a near constant behavior with spin along yrast band, indicating change of the nuclear shape in ^{188}Pt at low spins. The average absolute $\beta_2 = 0.20(3)$ obtained from measured B(E2) values matches well the values predicted by CHFB and IBM calculations for oblate ($\beta_2 \sim -0.19$) and prolate ($\beta_2 \sim 0.22$) shapes.

DOI:10.5506/APhysPolB.48.337

1. Introduction

The most common nuclear shape phenomena observed in nuclei of mass $A \sim 190$ are the shape coexistence and shape transition. A detailed review of shape coexistence in mass $A \sim 190$ is being given in a recent article by Heyde *et al.* [1]. For Pt nuclei, the theoretical calculations [2] for mass $A = 172$–194, suggest the shape transition rather than the shape coexistence. The calculations predict strongly deformed prolate shapes for low

* Presented at the Zakopane Conference on Nuclear Physics "Extremes of the Nuclear Landscape", Zakopane, Poland, August 28–September 4, 2016.

mass Pt nuclei ($A = 172$–186) but triaxial or rather oblate deformed shapes for heavier nuclei with $A = 188$–194. The signature of this trend of shapes change in Pt isotopes has been observed in the isotopic shift measurements by Roussiére *et al.* [3] and Lee *et al.* [4]. The calculations also predict ^{188}Pt as a transition point nucleus in this prolate-to-oblate shape change in Pt nuclei. Experimental results seem to support predictions as the lifetime measurements in neutron deficient even–even Pt nuclei with mass $A \leq 186$ [5–7] yielded high value of transitional quadrupole moment ($Q_{\mathrm{t}} \sim 7.23$–$5.6\,e$b) for these nuclei. In the case of ^{188}Pt, the calculations suggest that since both potential minima, corresponding to prolate ($\beta_2 = 0.22$) and oblate ($\beta_2 = -0.19$) shapes, exist in ground state, so the nucleus can be either prolate or oblate in the ground state. The recent spectroscopic measurements [8] tend to support near prolate deformed structure for this nucleus in (or near) the ground state. The measurements also show evolution of structure along yrast band from triaxial shape at intermediate spins to oblate shape at high spins for this nucleus. A sudden change of shape from prolate to oblate due to $\nu i_{13/2}$ neutron pair alignment is also predicted [9] between 10^+–12^+ state along the yrast band in this nucleus. From the measurement of level lifetimes, the transition quadrupole moment can be extracted, which is a measure of deformation in nuclei. Thus, the lifetime measurements have been carried out in ^{188}Pt with the recoil distance Doppler shift technique.

2. Experimental details

The high spin states in ^{188}Pt were populated via fusion-evaporation reaction $^{174}\mathrm{Yb}(^{18}\mathrm{O}, 4n)$ at a beam energy of 79 MeV. For this purpose, the good quality ^{18}O beam was delivered by 15 UD Pelletron accelerator at Inter University Accelerator Center (IUAC), New Delhi. This incident beam imparted recoil velocity $v/c \sim 0.8\%$ of the compound nucleus in the forward direction. For the experiment, the enriched ^{174}Yb target of thickness $\sim 750\,\mu\mathrm{g/cm}^2$, on a thick Ta backing foil of thickness $\sim 3\,\mathrm{mg/cm}^2$, was made by evaporation technique [10]. For a stopper, a self supporting thick Au foil of thickness $\sim 8\,\mathrm{mg/cm}^2$ was used. Both target and stopper foils were properly mounted and well-stretched on two identical metal cones placed opposite to each other in the RDM plunger setup available at IUAC [11] with target foil facing the beam. To find the minimum distance between target and stopper foils, the distance calibration was done by the capacitance method [12]. From the extrapolation of the plot of distance *vs.* capacitance^{-1}, minimum distance between target and stopper foils (d_0) was found to be $\sim 5\,\mu$m. A variation of $\pm 1\,\mu$m was observed due to target heating by the beam. In the experiment, the data was collected at 22 target–stopper distances ($d_{\mathrm{T-S}}$) ranging from 5 to 10 000 μm. For detection of emitted γ rays, the Gamma Detector Array

(GDA) setup available at IUAC, was used [11]. However, at the time of experiment, 6 detectors were used, so the data was taken with 4-detectors in the backward ring (144°) and 2-detectors in the forward ring (50°) in the GDA array. In addition to 6 HPGe detectors, the GDA had a BGO multiplicity filter array consisting of 14-BGO crystals, placed above and below the target chamber. The data was collected in the singles mode with the condition that at least two BGO crystals should fire ($M \geq 2$) in coincidence with one HPGe detector.

2.1. Data analysis and results

For analysis, singles data obtained with all four (two) detectors at backward (forward) angle after software gain matching, were added together and two raw spectra corresponding to the detectors at 50° and 144° were produced. A portion of the resulting energy spectrum at three target–stopper distances, obtained with detectors at backward angle is shown in Fig. 1.

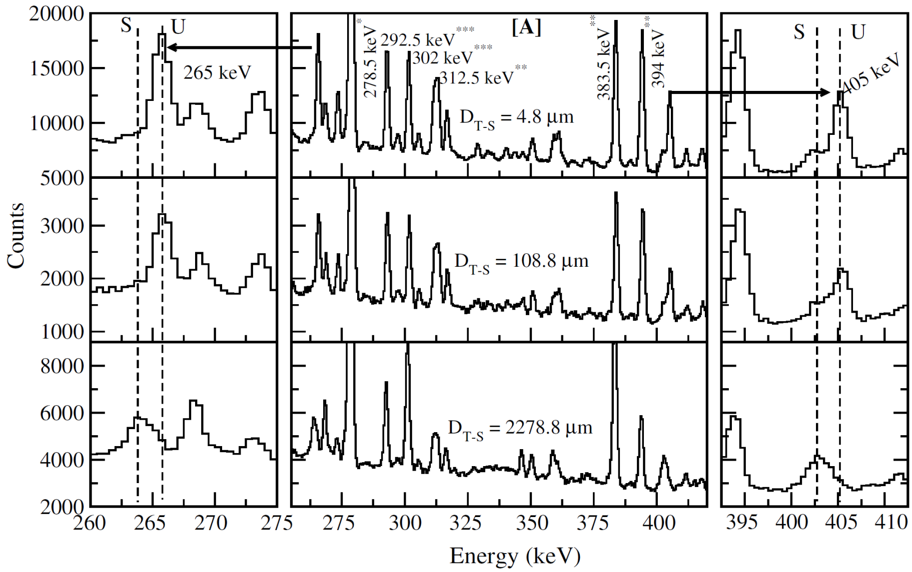

Fig. 1. [A]. Portion of raw spectra, showing all γ-ray transitions of interest of the yrast band in ^{188}Pt at three different target–stopper distances ($D_{\mathrm{T-S}}$) at an angle of 144° with respect to beam direction. For two lowest γ-ray transitions; 265 keV ($2^+ \to 0^+$) and 405 keV ($4^+ \to 2^+$), the shifted (S) and unshifted (U) peaks are clearly marked in the side panel of Fig. [A]. ($\star \to$ Coulex from ^{197}Au, $\star\star \to \gamma$ ray from $^{181}\mathrm{Ta}(^{18}\mathrm{O}, 4n\gamma)^{195}\mathrm{Tl}$ (Ta is the backing material in the target), $\star\star\star \to \gamma$ ray from $^{174}\mathrm{Yb}(^{18}\mathrm{O}, 5n\gamma)^{187}\mathrm{Pt}$).

In the present measurements, shifted (S) and unshifted (U) components of γ-ray transitions up to spin 12^+ in the yrast sequence were identified. For the analysis purpose, backward angle detector's spectra at each target–stopper distance were fitted to obtain areas of shifted and unshifted peaks (wherever possible). The obtained areas after applying the efficiency correction resulted in the intensity of unshifted (U) and shifted (S) γ-ray energy. The unshifted intensities have been normalised to 136 keV γ-ray (Coulex of ^{181}Ta) intensity at each distance. Normalized intensity of unshifted γ-ray transitions are then analyzed by the computer program LIFETIME [13]. In the simplest possible approach, the decay of levels along a cascade can be represented by a set of coupled differential equations, called Bateman's equations [14]. The program determines level population by direct solution of these Bateman equations and calculates values of shifted and unshifted intensities for each γ-ray transition. The finer details of the data analysis and various corrections applied are given in [11]. To find the error in the fitted parameters, the LIFETIME program includes a subroutine MINUIT [15] which calculates errors in the fitted parameters by examining behavior of χ^2-function over the unit interval on both sides of minimum.

3. Discussion of results

Looking at the results shown in Fig. 2, we observe that the experimental B(E2) values initially show an increasing behavior with spin up to 4^+ state but then show a nearly constant behavior at higher spins in ^{188}Pt. This is an indication of changing structure with spin in ^{188}Pt nucleus. As in ^{188}Pt, the increase of B(E2) values from $2^+ \to 4^+$ is more gradual than sharp

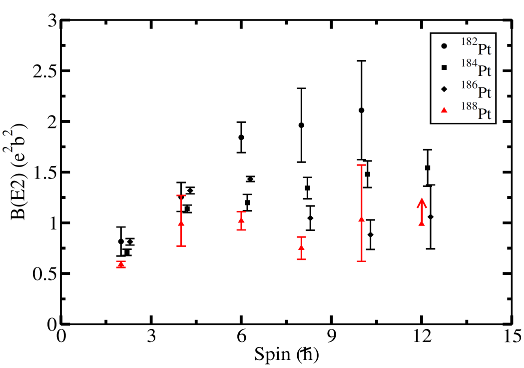

Fig. 2. The comparison of $B(\mathrm{E2}\!\downarrow)$ values for even-$A^{182,184,186}$Pt isotopes [5, 7] and the ^{188}Pt nuclei as a function of spin. To make the points non-overlapping and clear, the data for ^{184}Pt and ^{186}Pt have been plotted with spin offsets of $0.2\,\hbar$ and $0.3\,\hbar$ respectively.

(considering error bars) and constant thereafter, so the band mixing scenario, suggested for ^{182,184,186}Pt nuclei [7], does not fit well for this nucleus. However, when compared with the theoretical B(E2) values calculated using triaxial projected shell model [16] for ^{188}Pt nucleus, the experimental values show a good agreement with the calculations suggesting an increase in axial deformation of the nucleus for spins $2^+ \to 4^+$ in ^{188}Pt. In order to look into the issue of $A = 188$, as the transition point in prolate–oblate shape transition Pt isotopes, we plotted the average experimental Q_t values of even–even Pt isotopes, with mass $A = 182$–188. As shown in Fig. 3, the plotted Q_t values clearly demonstrate changing nuclear shape in Pt nuclei. Up to mass $A = 184$, experimentally and theoretically, the Pt nuclei have been well-established as having axially deformed prolate shapes. Beyond $A = 182$, the average experimental Q_t values in Pt are found to decrease with mass, with lowest value ($Q_t = 5.4 \pm 0.6\,e$b) obtained for ^{188}Pt. The decreasing Q_t values indicate reducing axial prolate collectivity in Pt nuclei towards higher mass. The absolute quadrupole deformation parameter $\beta_2 = 0.20 \pm 0.03$, corresponding to average $Q_t = 5.4 \pm 0.6\,e$b, obtained for ^{188}Pt in the present measurements, matches well with the magnitude of quadrupole deformation predicted by the CHFB and the IBM models for oblate ($\beta_2 \sim -0.19$) and for prolate ($\beta_2 \sim 0.22$) deformed shape of ^{188}Pt [2].

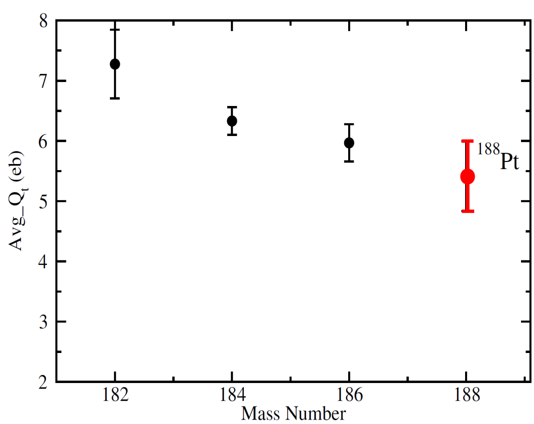

Fig. 3. The comparison of average experimental Q_t values for even mass Pt isotopes ($A = 182$–188) with mass number. To find average, the Q_t values for $2^+ \to 12^+$ states have been used. For ^{182}Pt, ^{184}Pt and ^{186}Pt, the data has been taken from reference [5, 7] respectively.

4. Summary and conclusions

In the present work, the prolate–oblate shape transition phenomenon in Pt nuclei has been investigated by measuring lifetimes and extracting deformation (in model-dependent way) in ^{188}Pt via the RDM lifetime measurement technique. The average absolute $\beta_2 = 0.20(3)$ obtained from measured B(E2) values matches well the values predicted by CHFB and IBM calculations for oblate ($\beta_2 \sim -0.19$) and prolate ($\beta_2 \sim 0.22$) shapes.

This work was supported in part by the Science and Education Research Board, India, under grant No. SB/S2/HEP-008/2013 and by the Research and Development grant of the University of Delhi, Delhi.

REFERENCES

[1] K. Heyde, J.L. Wood, *Rev. Mod. Phys.* **83**, 1467 (2011) and references therein.

[2] J.E. García *et al.*, *Phys. Rev. C* **89**, 034313 (2014).

[3] B. Roussiére *et al.*, *Hyperfine Interact.* **43**, 478 (1988).

[4] J.K.P. Lee *et al.*, *Phys. Rev. C* **38**, 2985 (1988).

[5] U. Garg *et al.*, *Phys. Lett. B* **180**, 319 (1986).

[6] G.D. Dracoulis *et al.*, *J. Phys. G* **12**, L97 (1986).

[7] J.C. Walpe *et al.*, *Phys. Rev. C* **85**, 057302 (2012).

[8] S. Mukhopadhyay *et al.*, *Phys. Lett. B* **739**, 462 (2014).

[9] L. Yuan *et al.*, *Chin. Phys. Lett.* **25**, 1633 (2008).

[10] Aman Rohilla *et al.*, *Nucl. Instrum. Methods Phys. Res. A* **797**, 230 (2015).

[11] S.K. Chamoli, *Nuclear Structure Study at High Spins*, LAP Lambert Academic Publishing, 2012, ISBN-978-3-8473-7018-5.

[12] T. Alexander, A. Bell, *Nucl. Instrum. Methods* **81**, 22 (1970).

[13] J.C. Wells, M.P. Fewell, N.R. Johnson, ORNL/TM-9105, 1985, DOI: 10.2172/6371400.

[14] R. Clark, N. Rowley, *J. Phys. G* **18**, 1515 (1992) and references therein.

[15] F. James, M. Ross, *Comput. Phys. Commun.* **10**, 343 (1975).

[16] G.H. Bhat *et al.*, *Phys. Rev. C* **86**, 047307 (2012).